

## Fabrication of Urchin-like Bismuth Nanostructures via a Facile Solvothermal Route

Chunjuan Tang, Y. X. Zhang, Guozhong Wang, H. Q. Wang, and Guanghai Li\*

Anhui Key Laboratory of Nanomaterials and Nanotechnology, Institute of Solid State Physics, Chinese Academy of Sciences, P. O. Box 1129, Hefei 230031, P. R. China

(Received April 15, 2008; CL-080391; E-mail: ghli@issp.ac.cn)

A facile solution-phase process has been demonstrated for the preparation of urchin-like bismuth nanostructures by reducing bismuth nitrate with ethylene glycol. X-ray diffraction (XRD), field emission scanning electron microscopy (FESEM), transmission electron microscopy (TEM), and selected area electron diffraction (SAED) have been used to characterize the as-prepared products. The formation mechanism has been proposed.

Fabrication of nanoscale inorganic crystals with controlled size, shape, and hierarchy has attracted intensive research interest, since they are potential building blocks for advanced electronic and optoelectronic devices.<sup>1</sup> Size- and shape-controlled synthesis of nanocrystal materials is a crucial issue for the exploitation of their novel properties. Extensive work has been devoted to the investigation of effective and efficient methods to fabricate one-dimensional (1D) nanostructures such as nanowires,<sup>2</sup> nanobelts,<sup>3</sup> and nanotubes<sup>4</sup> in the past few years. Compared to 1D nanostructures, complex three-dimensional (3D) architectures, such as branched  $\text{Cu}_2\text{O}$  crystals,<sup>5</sup> hierarchical structures from the self-assembly of polyhedral mesosphere crystals,<sup>6</sup> tetragonal  $\text{PbWO}_4$  microcrystals,<sup>7</sup> and hyperbranched  $\text{CdTe}$  and  $\text{CdSe}$  with rich 3D structures,<sup>8–11</sup> may offer opportunities to explore novel properties of nanocrystals and be employed as novel building blocks to produce more complicated and advanced nanomaterials.

As a semimetal with a small band overlap (38 meV at 5 K) with a very anisotropic electron effective-mass tensor, bismuth has unusual electronic properties and holds promise for optical and thermoelectric applications.<sup>12,13</sup> Different methods have been developed to fabricate bismuth nanomaterials in the form of nanotubes,<sup>14,15</sup> nanowires,<sup>16</sup> triangular nanoplate,<sup>17</sup> and nanowire arrays.<sup>18–20</sup> However, there is no report on the preparation of bismuth nanocrystals with 3D structures. It is necessary to explore a simple method to prepare bismuth with 3D nanostructures, which might have novel properties. In this letter, we reported the large-scale preparation of 3D structured bismuth nanocrystals with urchin-like morphology by a facile solvothermal method.

In a typical preparation process, 0.61 g of  $\text{Bi}(\text{NO}_3)_3 \cdot 5\text{H}_2\text{O}$  was dissolved into 50 mL of ethylene glycol (EG) at 80 °C. The solution was stirred vigorously for 1 h and transferred into a stainless steel autoclave with a Teflon liner. The autoclave was sealed and maintained at 180 °C for 10 h, then cooled to room temperature naturally. The obtained black solids were washed with deionized water and absolute ethanol for several times and dried in vacuum for 4 h.

XRD was used to determine the phase of the as-prepared product. All the diffraction peaks (Figure 1) can be indexed to hexagonal rhomb-centered phase bismuth (JCPDS card

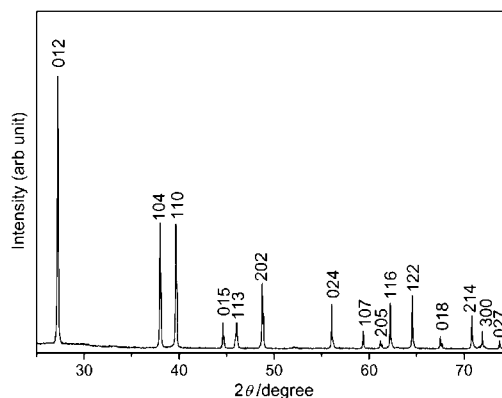


Figure 1. XRD pattern of bismuth prepared at 180 °C for 10 h.

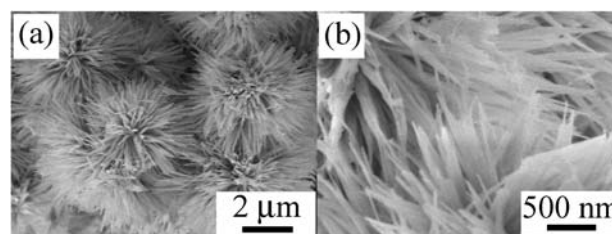
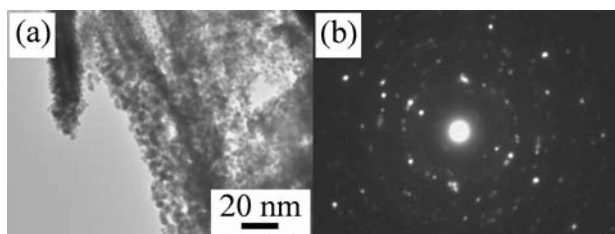


Figure 2. (a) Low- and (b) high-magnification FESEM images of bismuth prepared at 180 °C for 10 h.

No. 05-0519). No other diffraction peaks belonging to oxides or impurities can be observed in this pattern, indicating that the resulting product is highly crystallized elemental bismuth with high purity under current synthetic conditions.

The morphology of the as-prepared product was determined by FESEM. Figure 2a shows a low-magnification FESEM image of the product. Large-scale urchin-like bismuth nanostructures composed of many nanorods can be clearly seen. The urchin-like bismuth structures have the diameter of about 3  $\mu\text{m}$  with acicular nanorods radiating from the center and have nearly uniform size distribution. The yield of the urchin-like bismuth is about 85%. The high-magnification FESEM image shown in Figure 2b clearly demonstrates that the nanorods with diameter of about 20 nm grown from the center of the urchin and that some of the nanorods aligned together.

Figure 3a shows the TEM image of the bismuth nanorods. The urchin-like bismuth nanostructure is very sensitive to electron beam radiation because of very lower melting point of bismuth (271 °C). Once the electron beam was focused on them, the nanorods quickly became small bismuth liquid droplets. From Figure 3a, one can see that many small bismuth nanoparticles align into a nanorod shape. The analysis of the intrinsic structure for the nanorods is very difficult owing to their sensitiv-



**Figure 3.** (a) TEM image of the nanorods of urchin-like bismuth, and (b) the corresponding SAED.

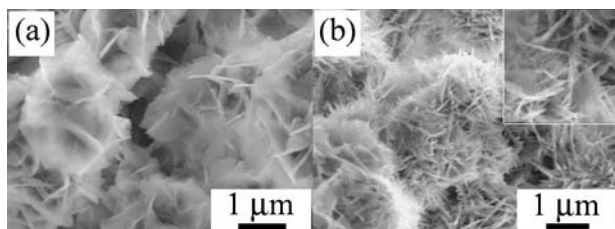
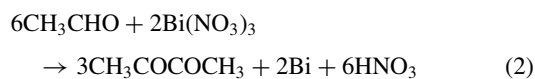
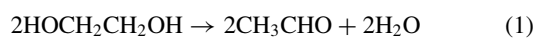


**Figure 4.** FESEM images of the products prepared at different times: (a) 1 and (b) 5 h.

ity to the electron beam radiation. The corresponding SAED pattern is shown in Figure 3b, in which the rings composed of spotty dots are from the nanoparticles.

To investigate the growth process of urchin-like bismuth, we carried out time-dependent experiments in which samples were collected at different time intervals from the reaction mixture once a precipitate appeared in the clear solution. Figure 4 shows the morphology evolution of urchin-like bismuth by collecting samples after reaction for 1 and 5 h. After reaction for 1 h, the product is nanospheres composed of nanoflakes (Figure 4a). As the reaction time was increased to about 5 h, there exist many short nanorods on the edge of the nanoflakes (inset of Figure 4b), and the product is still sphere-like (Figure 4b). After reaction for 10 h, the nanoflakes transform to the nanorods, as shown in Figure 2.

In the reaction, EG can coordinate with  $\text{Bi}^{3+}$ , which is similar to the role of ethylenediamine reported by Chen and his co-workers,<sup>21</sup> in which a typical coordinative reduction course is suggested. In this study, it is easy for EG to form dimers or trimers at high temperature, and then these dimers or trimers form lamellar structures with increasing temperature and pressure.<sup>22</sup> The reproducible process involved the reduction of  $\text{Bi}^{3+}$  with EG at 180 °C, and the chemical reaction can be formulated as



Based on the FESEM observations of the intermediate products, the formation mechanism of urchin-like bismuth can be described as follows: With the increase of temperature, the compound of EG and  $\text{Bi}^{3+}$  with a lamellar structure will self-assemble into nanospheres, and at the same time, the coordinative compound in the solution were reduced. The freshly crystallized particles are unstable because of the high surface

energy, and they tend to aggregate on the lamellar compound. With prolonged reaction time, the continuously formed bismuth particles served as the seeds for the growth of small nanorods at the expense of compound nanoflakes, and finally urchin-like bismuth structure was formed. Compared with the reported hydrothermal reduction of bismuth compounds in the literatures, our method is simple and controllable. EG serves not only as reducing agent but also as solvent, the reducibility of EG is relatively moderate and favors the orientation growth of the bismuth nanorods.

In conclusion, we have fabricated urchin-like bismuth nanostructures by a simple solvothermal method with a yield of about 85%. The novel structures should exhibit excellent electronic and thermoelectric properties, and further work is currently underway.

This work was financially supported by the National Natural Science Foundation of China (Grant No. 10704074).

## References

- 1 Y. Yin, A. P. Alivisatos, *Nature* **2005**, *437*, 664.
- 2 M. P. Zach, K. H. Ng, R. M. Penner, *Science* **2000**, *290*, 2120.
- 3 Z. W. Pan, Z. R. Dai, Z. L. Wang, *Science* **2001**, *291*, 1947.
- 4 L. Li, Y. Xiao, Y. Yang, X. Huang, G. Li, L. Zhang, *Chem. Lett.* **2005**, *34*, 930.
- 5 M. J. Siegfried, K.-S. Choi, *Adv. Mater.* **2004**, *16*, 1743.
- 6 Z. R. Tian, J. Liu, J. A. Voigt, B. McKenzie, H. Xu, *Angew. Chem., Int. Ed.* **2003**, *42*, 413.
- 7 B. Liu, S.-H. Yu, L. Li, Q. Zhang, F. Zhang, K. Jiang, *Angew. Chem., Int. Ed.* **2004**, *43*, 4745.
- 8 A. G. Kanaras, C. Sonnichsen, H. Liu, A. P. Alivisatos, *Nano Lett.* **2005**, *5*, 2164.
- 9 D. J. Milliron, S. M. Hughes, Y. Cui, L. Manna, J. Li, L.-W. Wang, A. P. Alivisatos, *Nature* **2004**, *430*, 190.
- 10 H. Liu, A. P. Alivisatos, *Nano Lett.* **2004**, *4*, 2397.
- 11 J. Tang, A. P. Alivisatos, *Nano Lett.* **2006**, *6*, 2701.
- 12 M. R. Black, Y.-M. Lin, S. B. Cronin, O. Rabin, M. S. Dresselhaus, *Phys. Rev. B* **2002**, *65*, 195417.
- 13 M. R. Black, P. L. Hagelstein, S. B. Cronin, Y. M. Lin, M. S. Dresselhaus, *Phys. Rev. B* **2003**, *68*, 235417.
- 14 Y. Li, J. Wang, Z. Deng, Y. Wu, X. Sun, D. Yu, P. Yang, *J. Am. Chem. Soc.* **2001**, *123*, 9904.
- 15 J. Wang, Y. Li, *Adv. Mater.* **2003**, *15*, 445.
- 16 H. Yu, P. C. Gibbons, W. E. Buhro, *J. Mater. Chem.* **2004**, *14*, 595.
- 17 R. Fu, S. Xu, Y.-N. Lu, J.-J. Zhu, *Cryst. Growth Des.* **2005**, *5*, 1379.
- 18 C. G. Jin, G. W. Jiang, W. F. Liu, W. L. Cai, L. Z. Yao, Z. Yao, X. G. Li, *J. Mater. Chem.* **2003**, *13*, 1743.
- 19 L. Li, Y. Zhang, G. Li, L. Zhang, *Chem. Phys. Lett.* **2003**, *378*, 244.
- 20 Y. Zhu, X. Dou, X. Huang, L. Li, G. Li, *J. Phys. Chem. B* **2006**, *110*, 26189.
- 21 Y. Gao, H. Niu, C. Zeng, Q. Chen, *Chem. Phys. Lett.* **2003**, *367*, 141.
- 22 P. R. Bonneau, R. F. Jarvis, Jr., R. B. Kaner, *Nature* **1991**, *349*, 510.